AD-A203 434 BURST GENERATION RATES IN SILICON AND GALLIUM ARSENIDE FROM NEUTRON-INDUC (U) SEVERN COMMUNICATIONS CORP SEVERNA PARK MD J R LETAW 15 AUG 87 SCC-87-02 1/1

UNCLASSIFIED N00014-87-C-2251 F/G 20/8 NL

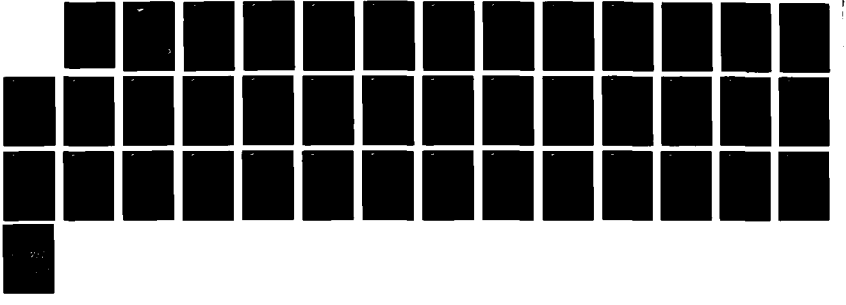

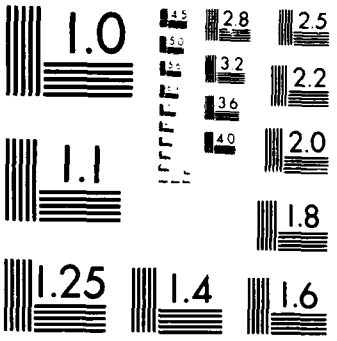

SCC Report 87 - 02

SEVERN COMMUNICATIONS CORPORATION

AD-A203 434

Burst Generation Rates In Silicon and Gallium Arsenide From Neutron-Induced Nuclear Recoils

15 August 1987

SEVERN COMMUNICATIONS CORPORATION
Box 544
Severna Park, Maryland 21146

Report Documentation Page

Report: SCC 87-02

Date: 15 August 1987

Title: Burst Generation Rates in Silicon and Gallium Arsenide from Neutron-Induced Nuclear Recoils

Author: John R. Letaw
Severn Communications Corporation
Box 544
Severna Park, MD 21146

Contract: #N00014-87-C-2251
Naval Research Laboratory
4555 Overlook Avenue, S.W.
Washington, DC 20375

Abstract: The HETC code (Los Alamos National Laboratory version) is used to estimate the energy spectra of residual nuclei in n-Si and n-GaAs reactions between 50 MeV and 1 GeV. A computation of the components of the burst generation rate from neutron-induced nuclear recoils between 1 MeV and 1 GeV is based on the Monte Carlo results and measured cross sections. These data may be applied to the computation of single-event upset rates from high-energy neutrons in the atmosphere and in spacecraft.

BURST GENERATION RATES

IN SILICON AND GALLIUM ARSENIDE

FROM NEUTRON-INDUCED NUCLEAR RECOILS

15 August 1987

Severn Communications Corporation
Box 544
Severna Park, Maryland 21146

TABLE OF CONTENTS

INTRODUCTION

Ziegler and Landford [1] introduced the concept of burst generation rate to quantify energy deposition by protons and neutrons in semiconductors. Concentrated bursts of energy (and therefore charge) occur in these materials as a result of relatively infrequent nuclear collisions. Tsao et al. [2] have pointed out that the charge deposition by nuclear fragments in high-energy collisions was omitted in [1] leading to an underestimate of the burst rate. The burst generation rate in GaAs, a semiconductor which offers the prospect of very-high speed curcuitry [3], has not been considered previously.

In this report we consider the nuclear recoil spectra from neutron interactions in Si and GaAs. Three separate methodologies are applied:

(1) At energies between 50 MeV and 1 GeV the recoil spectra are obtained from the HETC program.

(2) For low-energy bursts at neutron energies between 1 MeV and 20 MeV, the total and elastic scattering cross sections, and reaction kinematics, are used to estimate the recoil spectra.

(3) For high-energy bursts at neutron energies between 1 MeV and 20 MeV, specific inelastic cross sections and reaction kinematics are used to estimate the recoil spectra.

The recoil spectra are converted into burst generation rates using the formula:

$$B(E_n, E_b)\ \text{mb} = 4.99 \times 10^{-17}\sigma\ (\text{mb}) \qquad \text{Si}$$

$$4.43 \times 10^{-17}\sigma\ (\text{mb}) \qquad \text{GaAs}$$

where E_n is the incident neutron energy, E_b is the minimum recoil energy, and σ is the cross section for production of recoils exceeding E_b.

The present report does not consider the contribution of light, evaporated particles or gamma rays to the burst generation rate. Nuclear reaction cross sections and angular distributions are not available for some inelastic reactions. These reactions are not considered in this report. The energy of nuclear reaction products, with the exception of the nuclear recoil, is also not considered.

Burst generation rates make possible an estimate of the relative sensitivity of Si and GaAs devices to neutron-induced single-event upsets. The atmosphere, spacecraft with thick shielding, and the environment surrounding nuclear explosions contain neutrons. Any conclusions regarding the sensitivity of electronic systems in these environments must take into account the conversion factor between energy and charge deposition, the intrinsic speed of the devices, device feature sizes, and the spectrum of neutrons. Each of these factors may be of importance in determining the relative sensitivity of Si and GaAs devices to single-event upsets.

HETC RESULTS

The Los Alamos National Laboratory version of HETC [4] has been applied to compute the nuclear recoil spectra from interactions of neutrons in Si and GaAs at energies of 50, 70, 100, 150, 200, 300, 500, 700, and 1000 MeV. The differential recoil spectra are tabulated in Table 1 (Si) and Table 3 (GaAs), and plotted as histograms in Figures 1 through 9. Statistical uncertainties in this Monte Carlo computation may be estimated from the number of events in each energy bin (tabulated in Tables 2 and 4, for Si and GaAs respectively).

Burst generation rates are derived from the HETC results and tabulated in Table 5 (Si) and Table 6 (GaAs). The burst generation rates are plotted in Figure 10 (Si) and Figure 11 (GaAs) for burst energies of 0.03, 0.3, 1, 2, 3, 5, 7, 10, 12, and 15 MeV. Burst rates which are less than 3×10^{-17} cm^2/um^3 are not statistically significant and are not plotted. The rate for 10 MeV bursts from 300 MeV neutrons in GaAs appears anomalously low and is doubled in the plot.

TABLE 1

DIFFERENTIAL RECOIL SPECTRUM FOR NEUTRONS ON SILICON (mb/MeV)

Recoil Energy (MeV[a])	Neutron Energy (MeV) 50	70	100	150	200	300	500	700	1000
0.0100	188.	135.	135.	115.	115.	104.	52.	125.	135.
0.0147	466.	355.	200.	244.	133.	177.	244.	155.	333.
0.0215	306.	291.	276.	169.	123.	184.	215.	153.	245.
0.0316	444.	402.	361.	175.	165.	206.	268.	217.	206.
0.0464	472.	408.	458.	317.	246.	317.	289.	289.	317.
0.0681	466.	499.	543.	379.	288.	312.	384.	442.	423.
0.100	532.	447.	431.	385.	359.	330.	431.	451.	474.
0.147	545.	537.	397.	335.	330.	308.	448.	565.	517.
0.215	518.	397.	377.	366.	297.	270.	325.	380.	363.
0.316	479.	387.	355.	294.	260.	247.	231.	255.	214.
0.464	424.	325.	264.	211.	228.	206.	201.	198.	170.
0.681	321.	264.	209.	191.	162.	184.	173.	160.	161.
1.00	241.	190.	163.	143.	146.	139.	136.	131.	122.
1.47	164.	138.	124.	93.8	92.7	98.2	82.5	84.0	81.6
2.15	98.4	95.0	76.5	65.7	67.1	59.0	64.7	60.7	58.5
3.16	42.2	48.4	46.1	41.8	41.6	41.7	36.1	41.8	43.6
4.64	12.5	17.4	20.4	22.7	21.2	22.2	25.4	28.2	28.1
6.81	1.92	4.80	6.58	10.2	11.0	10.3	14.5	17.7	18.2
10.0	0.16	0.46	1.44	2.91	4.41	5.26	7.38	8.88	9.15
14.7	0.00	0.04	0.13	0.64	1.04	1.18	2.86	3.26	3.53
21.5	0.00	0.00	0.02	0.08	0.14	0.35	0.80	1.06	1.64
31.6	0.00	0.00	0.00	0.00	0.00	0.04	0.14	0.25	0.30

[a] Upper limit of energy bin.

TABLE 2

NUMBER OF MONTE CARLO TRIALS IN

n-Si RECOIL SPECTRUM COMPUTATION

Recoil Energy (MeV[a])	Neutron Energy (MeV)								
	50	70	100	150	200	300	500	700	1000
0.0100	18	13	13	11	11	10	5	12	13
0.0147	21	16	9	11	6	8	11	7	15
0.0215	20	19	18	11	8	12	14	10	16
0.0316	43	39	35	17	16	20	26	21	20
0.0464	67	58	65	45	35	45	41	41	45
0.0681	97	104	113	79	60	65	80	92	88
0.100	163	137	132	118	110	101	132	138	145
0.147	246	242	179	151	149	139	202	255	233
0.215	338	259	246	239	194	176	212	248	237
0.316	464	375	344	285	252	239	224	247	207
0.464	602	462	375	300	324	293	286	281	242
0.681	669	550	436	397	337	383	360	333	335
1.00	737	583	498	438	447	426	416	400	374
1.47	740	624	561	423	418	443	372	379	368
2.15	642	620	499	429	438	385	422	396	382
3.16	409	469	447	405	403	404	350	405	423
4.64	177	247	290	322	301	316	361	401	399
6.81	40	100	137	212	229	214	302	369	380
10.0	5	14	44	89	135	161	226	272	280
14.7	0	2	6	29	47	53	129	147	159
21.5	0	0	1	5	9	23	52	69	107
31.6	0	0	0	0	0	4	14	24	29
Total[b]	5500	4934	4448	4022	3934	3944	4358	4814	4948

a Upper limit of energy bin.
b Total number of interactions in 10000 Monte Carlo trials.

TABLE 3

DIFFERENTIAL RECOIL SPECTRUM FOR NEUTRONS ON GALLIUM ARSENIDE (mb/MeV)

Recoil Energy (MeV[a])	Neutron Energy (MeV) 50	70	100	150	200	300	500	700	1000
0.0100	1176.	1084.	901.	687.	550.	504.	580.	626.	596.
0.0147	2404.	1527.	1300.	1430.	1040.	682.	877.	650.	812.
0.0215	2133.	1864.	1347.	1280.	1168.	1302.	1235.	1190.	1145.
0.0316	2147.	1935.	1739.	1542.	1497.	1164.	983.	1285.	1270.
0.0464	2311.	2002.	1661.	1321.	1475.	1455.	1362.	1486.	1527.
0.0681	1914.	1604.	1450.	1365.	1337.	1400.	1365.	1590.	1443.
0.100	1709.	1575.	1288.	1216.	1048.	905.	1034.	1096.	1063.
0.147	1553.	1368.	1189.	903.	812.	825.	650.	611.	614.
0.215	1403.	1098.	889.	714.	714.	716.	525.	478.	516.
0.316	1117.	877.	774.	627.	553.	600.	491.	463.	432.
0.464	944.	698.	589.	464.	445.	492.	392.	352.	317.
0.681	621.	545.	416.	401.	381.	304.	283.	261.	278.
1.00	376.	356.	347.	280.	284.	238.	241.	224.	190.
1.47	151.	202.	194.	202.	174.	172.	175.	179.	167.
2.15	39.1	74.6	104.	117.	117.	109.	121.	130.	111.
3.16	7.26	17.2	38.4	51.7	56.4	60.8	82.8	92.7	85.9
4.64	0.83	3.20	9.18	20.2	26.6	34.4	47.7	55.2	56.9
6.81	0.00	0.07	0.84	3.52	6.90	12.7	22.7	32.4	37.1
10.0	0.00	0.00	0.05	0.81	1.01	3.54	9.05	13.7	18.8
14.7	0.00	0.00	0.00	0.03	0.29	0.36	3.12	5.30	8.22
21.5	0.00	0.00	0.00	0.00	0.00	0.02	0.47	1.15	2.87
31.6	0.00	0.00	0.00	0.00	0.00	0.00	0.06	0.12	0.59

[a] Upper limit of bin energy.

TABLE 4

NUMBER OF MONTE CARLO TRIALS IN

n-GaAs RECOIL SPECTRUM COMPUTATION

Recoil Energy (MeV[a])	Neutron Energy (MeV)								
	50	70	100	150	200	300	500	700	1000
0.0100	77	71	59	45	36	33	38	41	39
0.0147	74	47	40	44	32	21	27	20	25
0.0215	95	83	60	57	52	58	55	53	51
0.0316	142	128	115	102	99	77	65	85	84
0.0464	224	194	161	128	143	141	132	144	148
0.0681	272	228	206	194	190	199	194	226	205
0.100	357	329	269	254	219	189	216	229	222
0.147	478	421	366	278	250	254	200	188	189
0.215	625	489	396	318	318	319	234	213	230
0.316	739	580	512	415	366	397	325	306	286
0.464	915	677	571	450	431	477	380	341	307
0.681	883	775	591	570	542	432	402	371	395
1.00	785	744	725	585	594	498	504	467	397
1.47	464	621	598	621	536	529	538	550	514
2.15	174	332	462	520	520	484	540	579	494
3.16	48	114	254	342	373	402	548	613	568
4.64	8	31	89	196	258	333	462	535	552
6.81	0	1	12	50	98	181	323	460	528
10.0	0	0	1	17	21	74	189	286	393
14.7	0	0	0	1	9	11	96	163	253
21.5	0	0	0	0	0	1	21	51	128
31.6	0	0	0	0	0	0	4	8	39
Total[b]	6361	5865	5487	5189	5088	5110	5493	5935	6053

a Upper limit of bin energy.
b Total number of interactions in 10000 Monte Carlo trials.

FIGURE 1

RECOIL SPECTRA FOR 50 MeV NEUTRONS ON Si AND GaAs

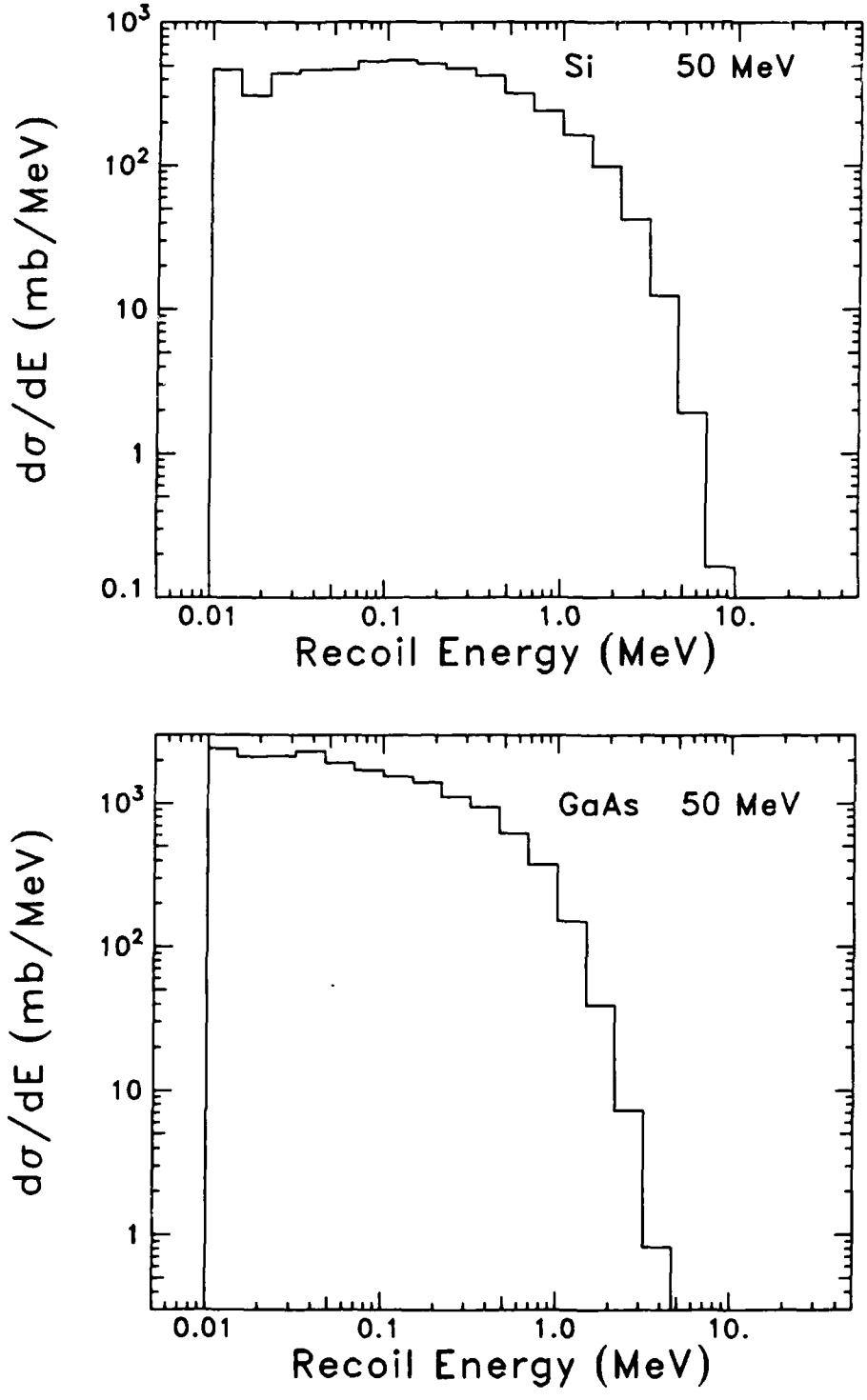

FIGURE 2

RECOIL SPECTRA FOR 70 MeV NEUTRONS ON Si AND GaAs

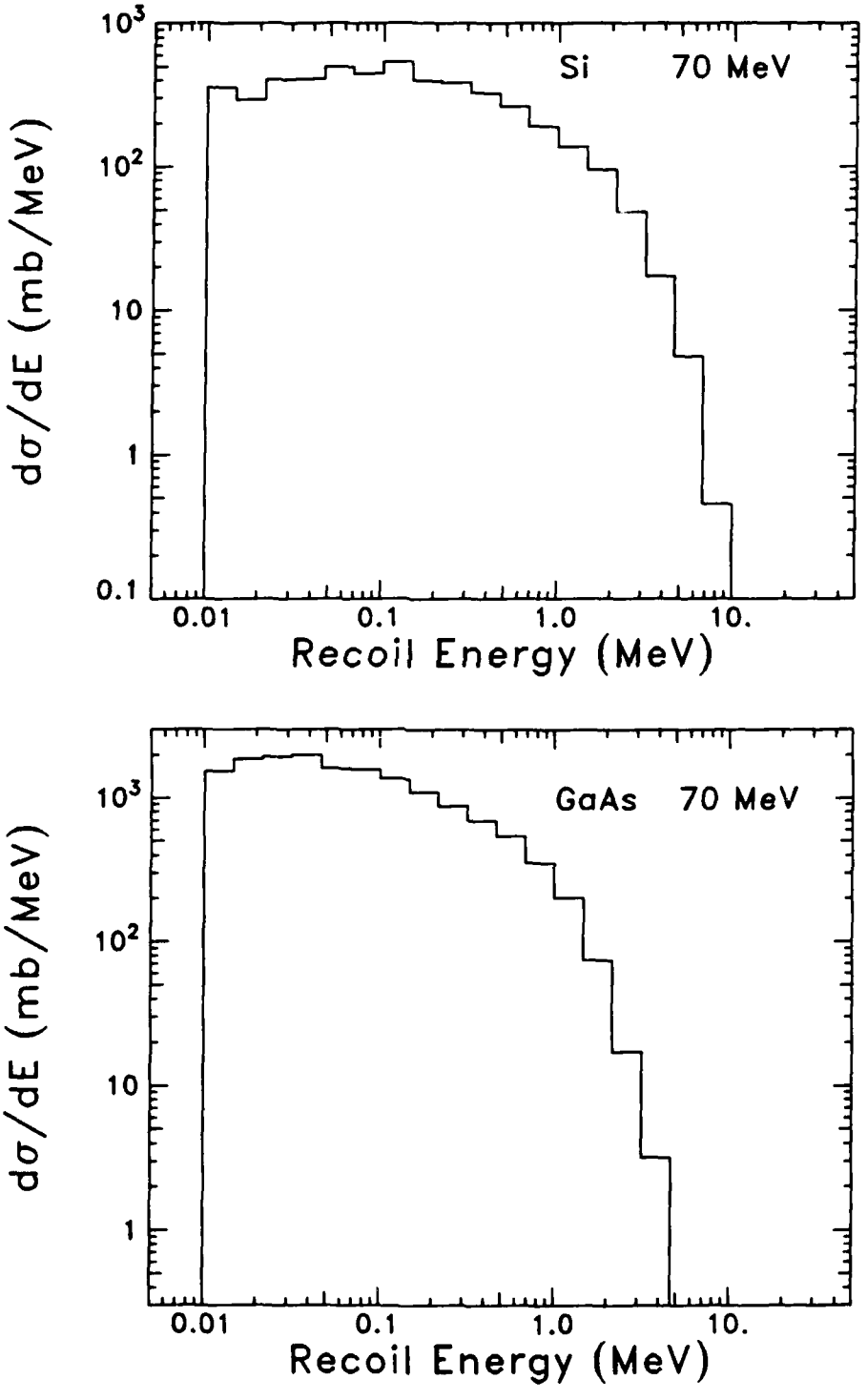

FIGURE 3

RECOIL SPECTRA FOR 100 MeV NEUTRONS ON Si AND GaAs

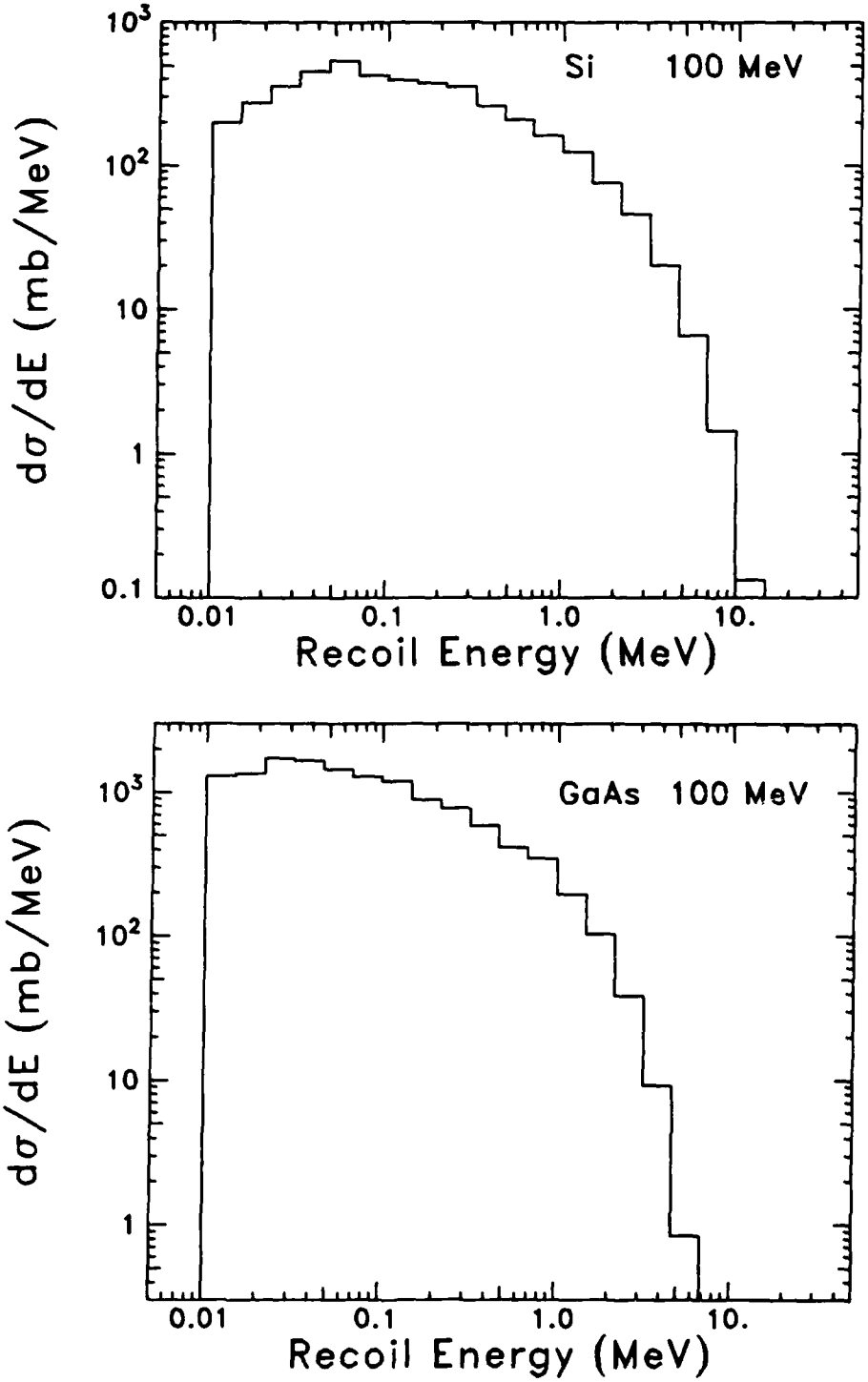

FIGURE 4

RECOIL SPECTRA FOR 150 MeV NEUTRONS ON Si AND GaAs

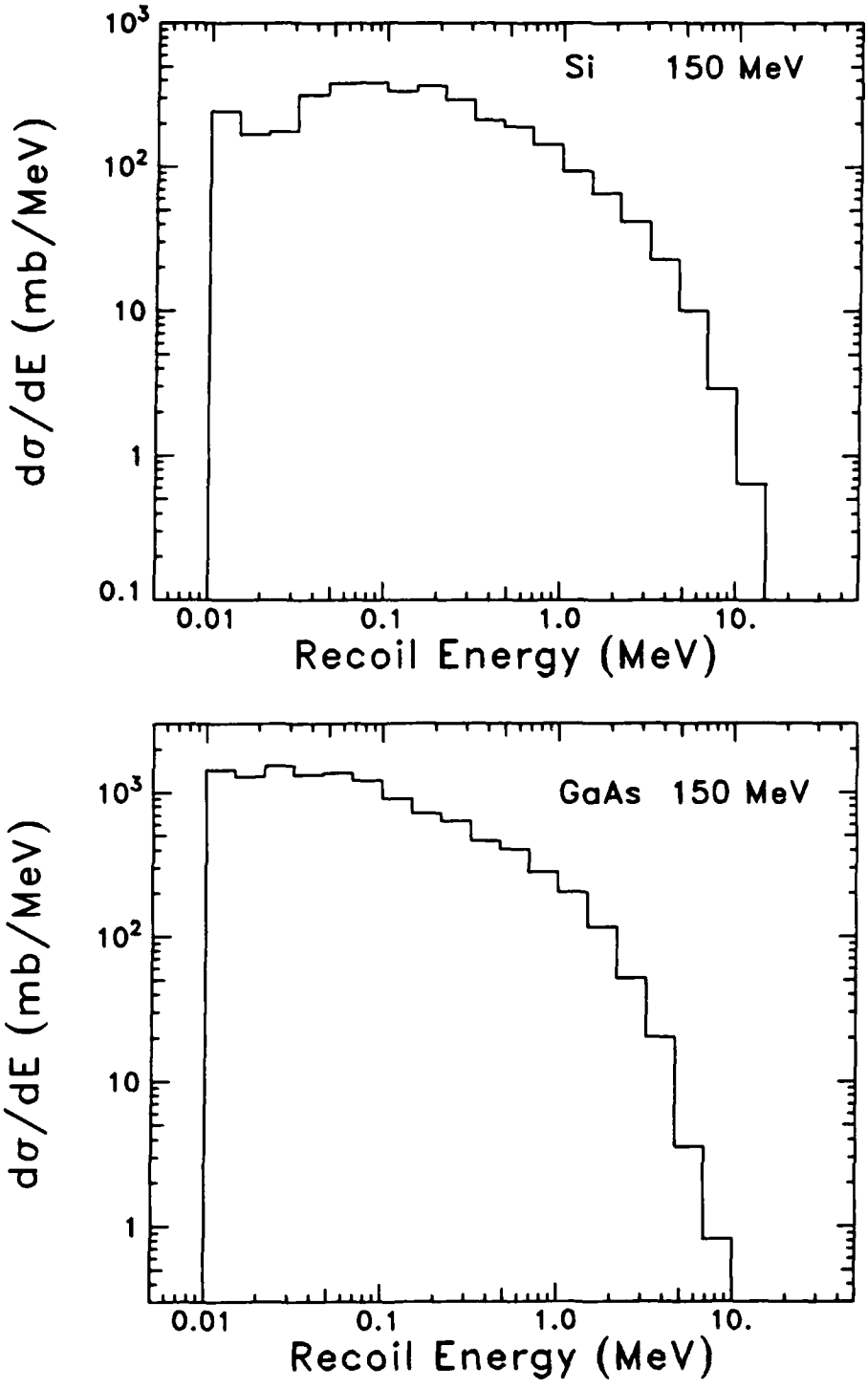

FIGURE 5

RECOIL SPECTRA FOR 200 MeV NEUTRONS ON Si AND GaAs

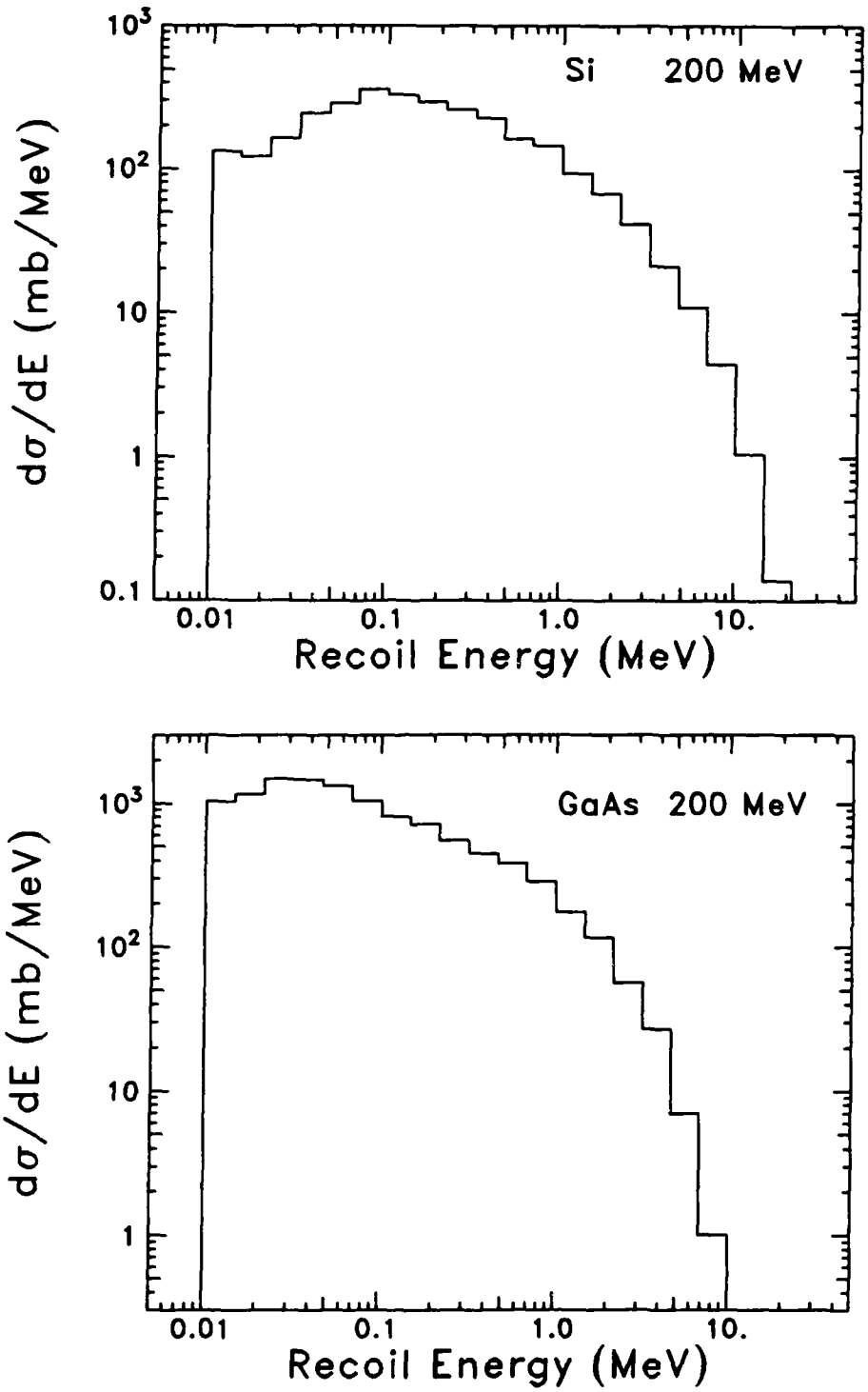

FIGURE 6

RECOIL SPECTRA FOR 300 MeV NEUTRONS ON Si AND GaAs

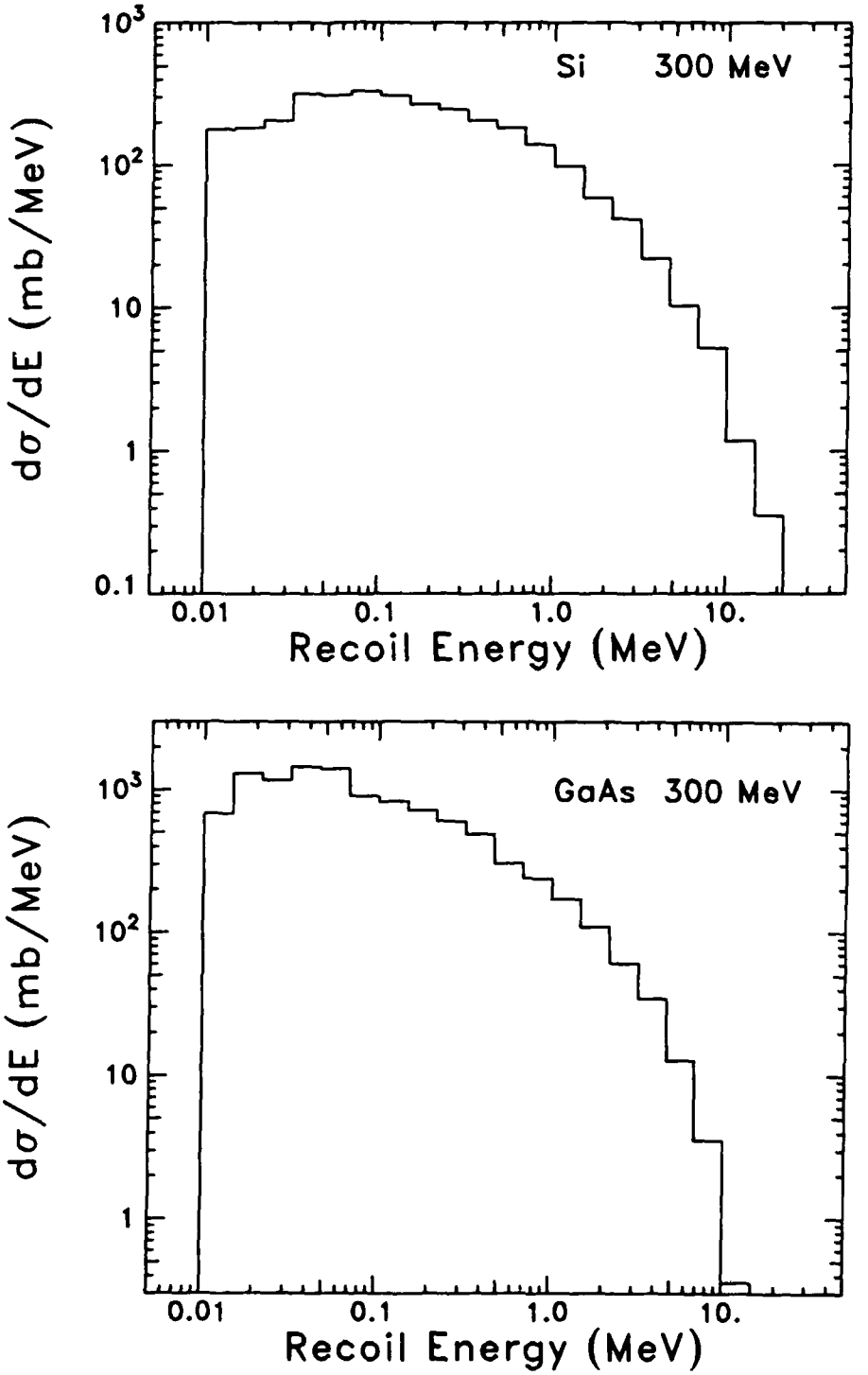

FIGURE 7

RECOIL SPECTRA FOR 500 MeV NEUTRONS ON Si AND GaAs

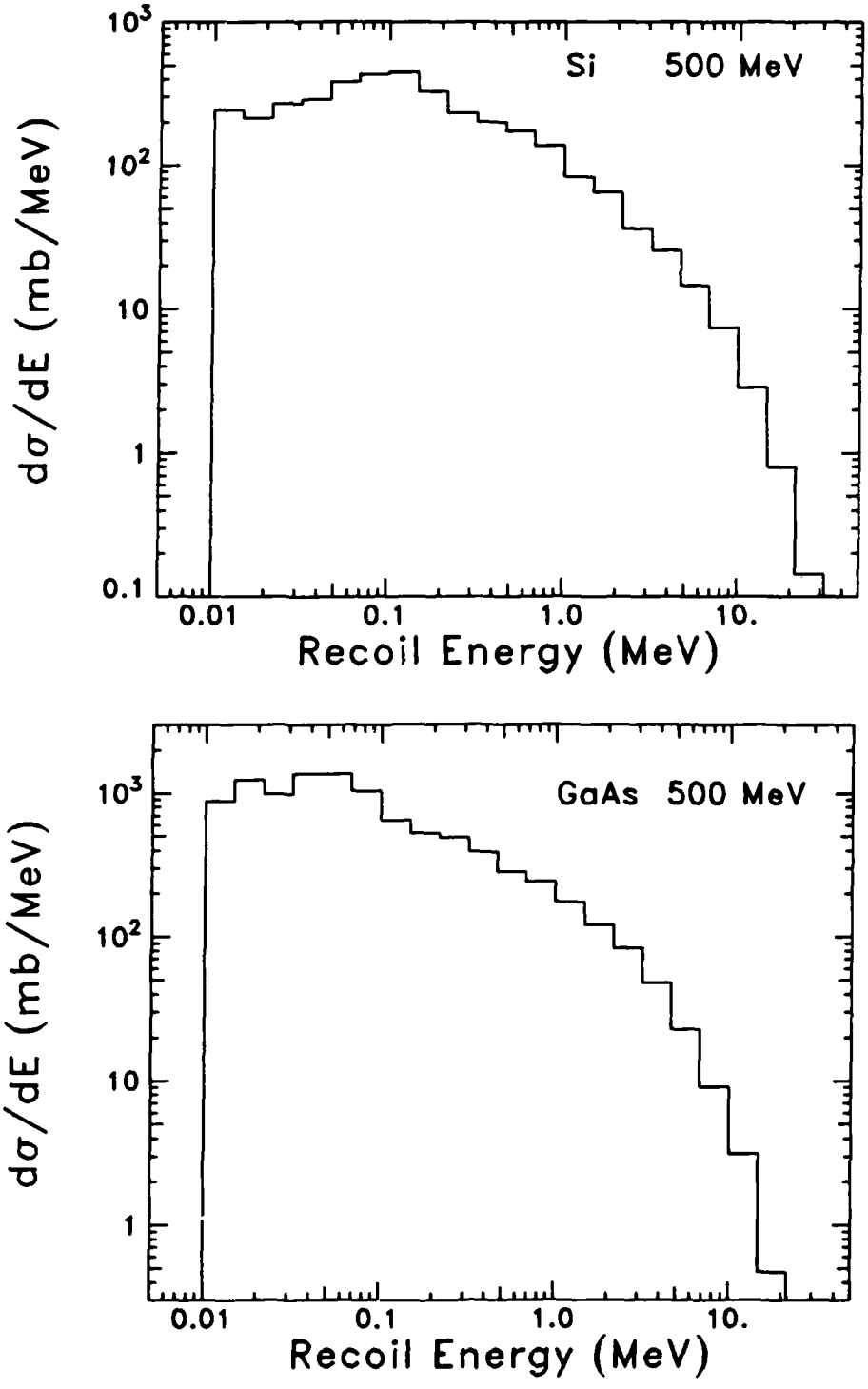

FIGURE 8

RECOIL SPECTRA FOR 700 MeV NEUTRONS ON Si AND GaAs

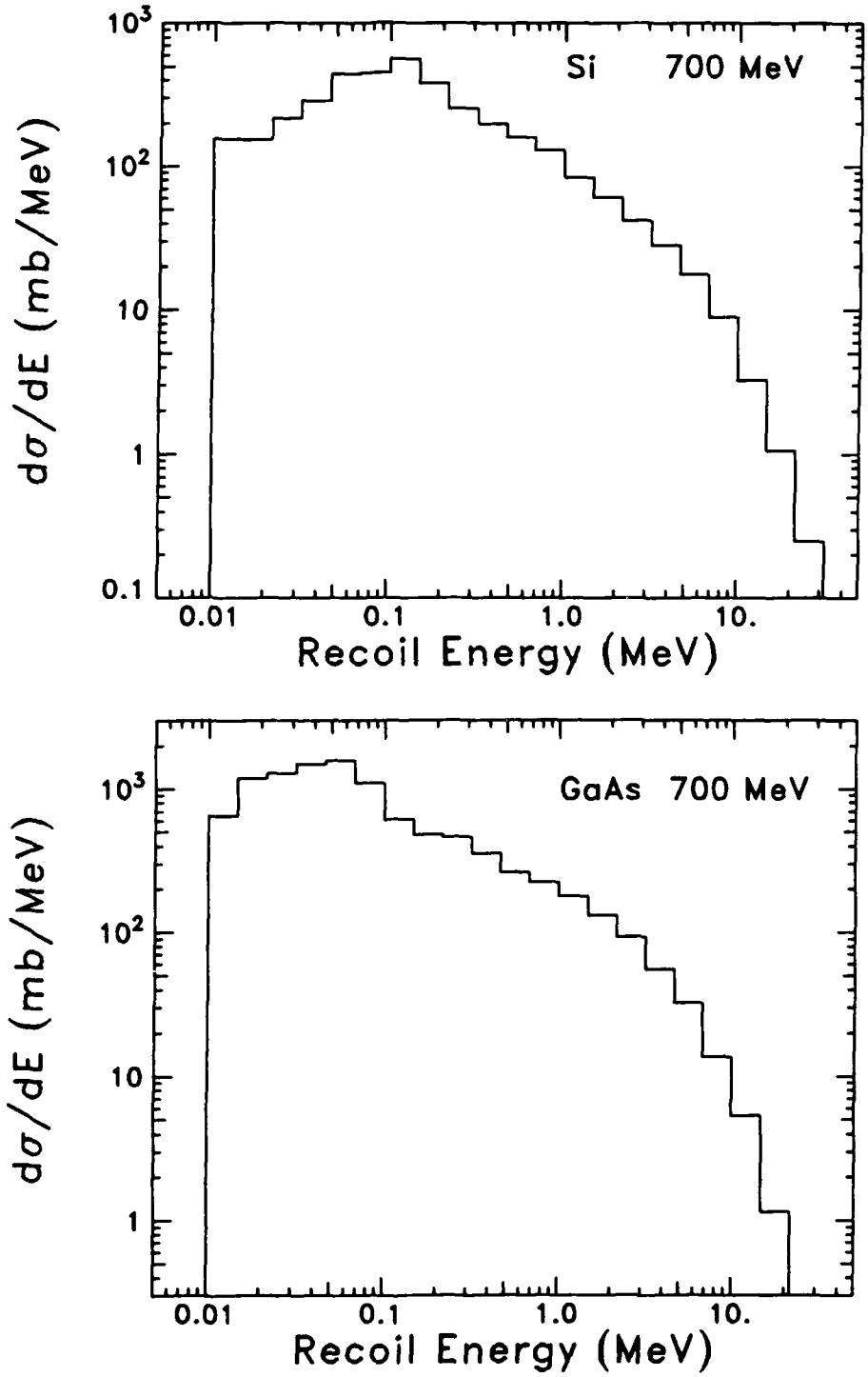

FIGURE 9

RECOIL SPECTRA FOR 1000 MeV NEUTRONS ON Si AND GaAs

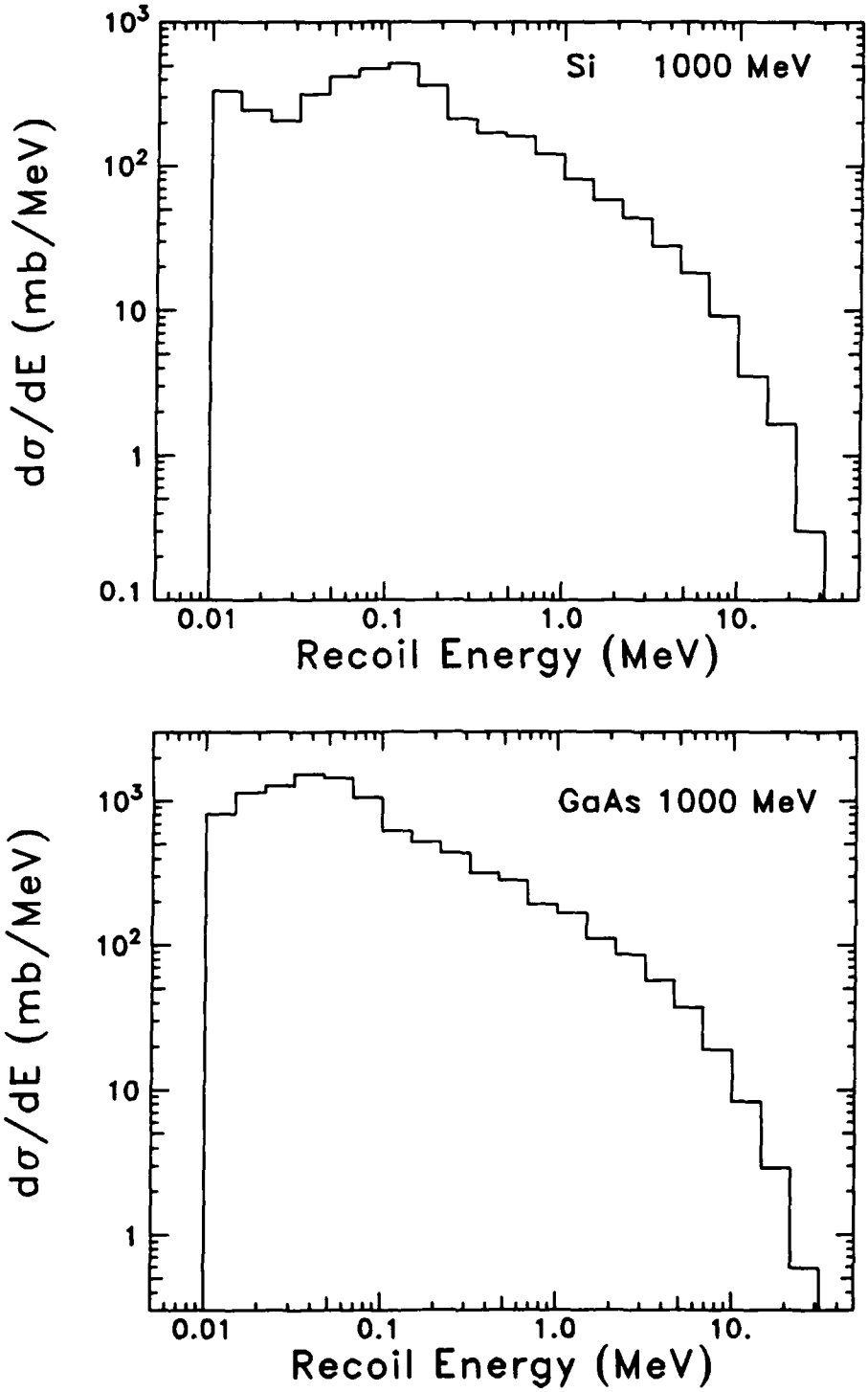

TABLE 5

BURST GENERATION RATE OF NEUTRONS ON SI

(Nuclear Recoil Component from HETC)

Burst Energy (MeV)	Neutron Energy (MeV)								
	50	70	100	150	200	300	500	700	1000
0.01	285.	256.	231.	208.	204.	203.	220.	236.	234.
0.02	283.	254.	229.	207.	203.	202.	219.	235.	232.
0.03	281.	252.	228.	206.	202.	201.	218.	234.	231.
0.05	276.	248.	223.	203.	200.	198.	215.	231.	228.
0.07	272.	243.	218.	200.	197.	195.	211.	227.	223.
0.10	264.	236.	211.	194.	191.	190.	204.	220.	217.
0.20	238.	213.	192.	176.	176.	176.	185.	196.	195.
0.30	213.	194.	174.	161.	162.	163.	172.	183.	182.
0.50	171.	162.	148.	139.	140.	144.	153.	163.	166.
0.70	140.	136.	127.	121.	125.	125.	136.	148.	150.
1.00	105.	108.	103.	99.5	103.	104.	116.	128.	132.
2.00	39.0	49.0	52.6	59.6	62.8	64.7	78.7	92.5	96.7
3.00	13.3	21.4	27.4	36.6	40.4	42.5	58.5	69.7	73.6
5.00	1.82	4.11	8.01	14.3	19.3	21.2	35.4	42.1	45.9
7.00	0.21	0.68	2.50	6.24	9.26	11.8	21.2	25.8	29.3
10.0	0.00	0.10	0.36	1.77	2.91	4.21	10.3	12.8	15.9
12.0	0.00	0.05	0.05	0.83	1.82	2.60	6.71	8.84	11.7
15.0	0.00	0.00	0.05	0.21	0.47	1.35	3.43	4.94	7.12

TABLE 6

BURST GENERATION RATE OF NEUTRONS ON GaAs

(Nuclear Recoil Component from HETC)

Burst Energy (MeV)	Neutron Energy (MeV)								
	50	70	100	150	200	300	500	700	1000
0.01	425.	392.	367.	348.	342.	344.	369.	398.	407.
0.02	415.	385.	362.	342.	336.	339.	364.	395.	402.
0.03	406.	375.	354.	335.	331.	334.	360.	389.	397.
0.05	386.	358.	340.	323.	318.	321.	348.	377.	383.
0.07	369.	345.	327.	311.	306.	309.	336.	362.	371.
0.10	346.	324.	310.	295.	292.	297.	322.	347.	357.
0.20	280.	269.	264.	259.	258.	263.	297.	323.	332.
0.30	229.	228.	229.	232.	233.	235.	274.	302.	313.
0.50	147.	167.	178.	189.	192.	194.	240.	272.	284.
0.70	95.8	121.	141.	155.	160.	167.	215.	249.	259.
1.00	46.9	74.4	95.8	118.	123.	136.	184.	220.	235.
2.00	4.74	13.2	28.4	46.8	57.0	72.8	118.	151.	174.
3.00	0.74	2.71	8.52	20.5	27.9	43.5	78.8	108.	133.
5.00	0.00	0.07	0.68	3.86	6.70	15.3	37.7	59.2	84.8
7.00	0.00	0.00	0.07	1.01	2.03	5.48	19.6	32.9	53.3
10.00	0.00	0.00	0.00	0.07	0.61	0.81	8.19	15.2	28.7
12.00	0.00	0.00	0.00	0.00	0.14	0.27	4.46	8.86	20.0
15.00	0.00	0.00	0.00	0.00	0.00	0.07	1.62	4.19	10.7

FIGURE 10

BURST GENERATION RATE OF NEUTRONS ON Si

(Nuclear Recoil Component from HETC)

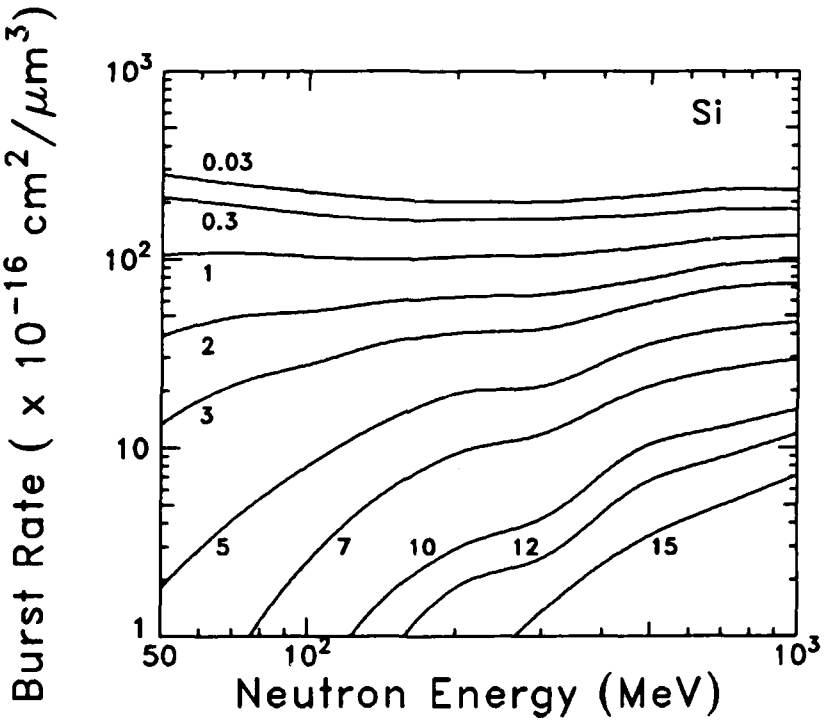

FIGURE 11

BURST GENERATION RATE OF NEUTRONS ON GaAs

(Nuclear Recoil Component from HETC)

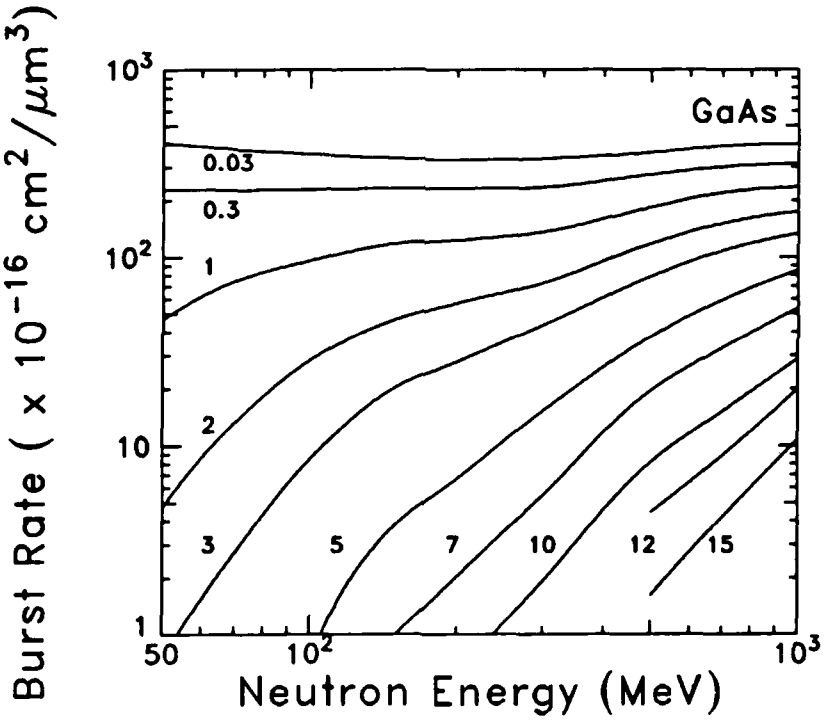

ELASTIC SCATTERING RESULTS

Elastic scattering of neutrons contributes to the low-energy bursts at neutron energies < 50 MeV. At higher energies inelastic reactions dominate the burst generation rate because they are the most probable reaction channels. At low energies the high-energy bursts are dominated by infrequent inelastic collisions because large momentum transfer is unlikely, both because of kinematics and the reaction mechanism, in elastic collisions.

Elastic scattering cross sections (< 20 MeV) from the ENDF data collection [5] are shown in Table 7. Reaction kinematics fully define the nuclear recoil energy if the center-of-mass scattering angle is known. The distribution of scattering angles has been measured in numerous experiments; however, due to time limitations we make the simplifying assumption that the elastic scattering angular distribution is isotropic.

The elastic scattering component of the burst generation rate is tabulated in Table 8 (Si) and Table 9 (GaAs), and is plotted in Figure 12 (Si) and Figure 13 (GaAs). The burst rate is nearly correct for the lowest energy bursts, but is overestimated by approximately a factor of two for large angle scattering. This conclusion is based on a comparison with [1] and a cursory analysis of elastic scattering angular distributions.

TABLE 7

ELASTIC SCATTERING CROSS SECTIONS

FOR NEUTRONS ON Si AND GaAs [a]

Energy (MeV)	Cross Section (mb) Si	GaAs
1	4037	3586
2	2310	1858
3	2310	1720
4	2154	2254
5	1630	2532
7	705	2632
10	705	2532
12	756	2342
15	811	1930
20	933	1786

[a] Natural gallium cross section was adopted.

TABLE 8

BURST GENERATION RATE OF NEUTRONS ON Si

(Elastic Scattering Component: Isotropic Assumption)

Neutron Energy (MeV)	Burst Energy (MeV) 0.03	0.10	0.3	1.0	2.0	3.0	5.0	7.0	10.0
1.	1556.	504.	0.	0.	0.	0.	0.	0.	0.
2.	1021.	721.	0.	0.	0.	0.	0.	0.	0.
3.	1065.	865.	288.	0.	0.	0.	0.	0.	0.
4.	1014.	872.	472.	0.	0.	0.	0.	0.	0.
5.	777.	692.	449.	0.	0.	0.	0.	0.	0.
7.	340.	314.	239.	0.	0.	0.	0.	0.	0.
10.	344.	325.	273.	89.	0.	0.	0.	0.	0.
12.	370.	354.	306.	143.	0.	0.	0.	0.	0.
15.	399.	384.	344.	204.	4.	0.	0.	0.	0.
20.	460.	448.	414.	293.	120.	0.	0.	0.	0.

TABLE 9

BURST GENERATION RATE OF NEUTRONS ON GaAs

(Elastic Scattering Component: Isotropic Assumption)

Neutron Energy (MeV)	Burst Energy (MeV) 0.03	0.10	0.3	1.0	2.0	3.0	5.0	7.0	10.0
1.	704.	0.	0.	0.	0.	0.	0.	0.	0.
2.	595.	64.	0.	0.	0.	0.	0.	0.	0.
3.	621.	292.	0.	0.	0.	0.	0.	0.	0.
4.	858.	538.	0.	0.	0.	0.	0.	0.	0.
5.	997.	706.	0.	0.	0.	0.	0.	0.	0.
7.	1072.	857.	244.	0.	0.	0.	0.	0.	0.
10.	1058.	914.	502.	0.	0.	0.	0.	0.	0.
12.	989.	879.	559.	0.	0.	0.	0.	0.	0.
15.	822.	750.	542.	0.	0.	0.	0.	0.	0.
20.	769.	718.	572.	70.	0.	0.	0.	0.	0.

FIGURE 12

BURST GENERATION RATE OF NEUTRONS ON Si

(Elastic Scattering Component: Isotropic Assumption)

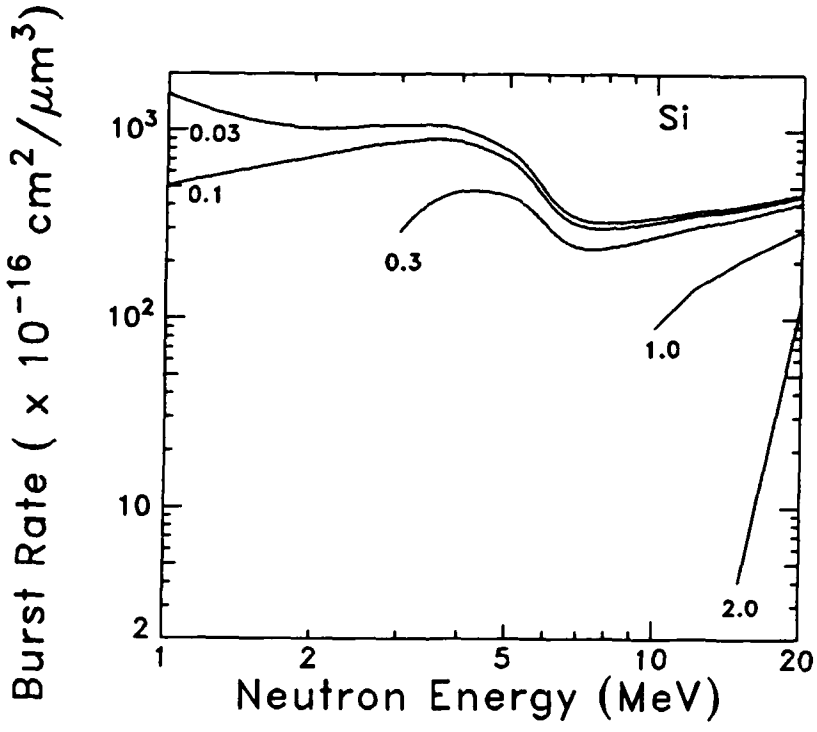

FIGURE 13

BURST GENERATION RATE OF NEUTRONS ON GaAs

(Elastic Scattering Component: Isotropic Assumption)

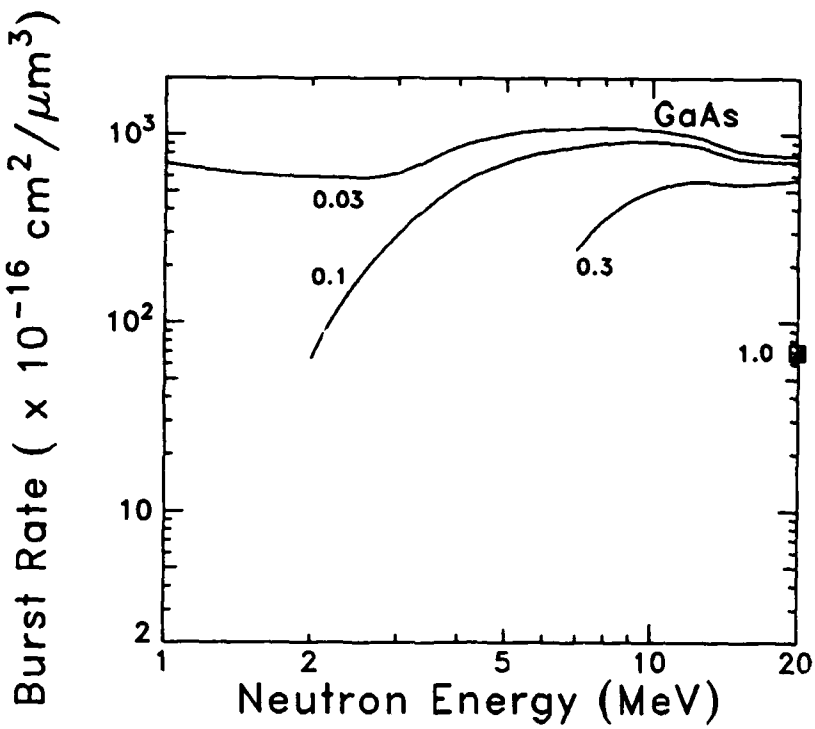

INELASTIC SCATTERING RESULTS

Inelastic scattering - particularly (n,α), (n,p), and (n,nX) reactions - is an important component of the burst generation rate for production of high-energy recoil nuclei. Inelastic collisions generally involve larger momentum transfers than elastic collisions. In addition, the threshold for any given burst energy is lower through inelastic channels than through elastic channels.

For non-relativistic elastic interactions the threshold neutron energy for bursts of energy E_b is:

$$E_n = 7.5\ E_b \quad \text{for Si}$$

$$18.6\ E_b \quad \text{for GaAs}$$

For inelastic interactions the threshold energy is generally lower (except when limited by binding energies). The threshold is not simply related to the burst energy for inelastic reactions. Table 10 (Si) and Table 11 (GaAs) show a comparison of neutron energy thresholds for various burst energies.

Table 12 shows the inelastic scattering cross sections used in this analysis. These cross sections were taken from the ENDF data collection [5]. (n,nX) reactions have not been considered in this analysis because time limitations do not allow a full analysis of kinematics and angular distribution. The (n,np), (n,nα), and (n,2n) reactions are important for neutrons on Si above 13 MeV. The (n,2n) reaction dominates the neutron inelastic interaction on GaAs between 11 MeV and 20 MeV. (n,nX) reactions must be included for an accurate estimate of inelastic burst generation rates between 11 MeV and 20 MeV.

The burst generation rates for inelastic scattering of neutrons on Si and GaAs are tabulated in Tables 13 and 14, respectively. An isotropic angular distribution of recoil nuclei has been assumed. This assumption is consistent with the compound nucleus model which is applicable (to some degree) for low-energy neutron interactions. The inelastic burst generation rates are shown in Figure 13 (Si) and Figure 14 (GaAs).

TABLE 10

THRESHOLD KINETIC ENERGY FOR SEVERAL BURST ENERGIES

FROM ELASTIC AND INELASTIC SCATTERING ON Si

	Neutron Energy Threshold (MeV)	
Burst Energy (MeV)	Elastic	Inelastic
0.03	0.23	2.7
0.1	0.75	2.7
0.3	2.3	3.2
1.	7.5	5.4
2.	15.1	8.8
3.	22.6	12.2
4.	30.	15.7
5.	38.	19.
7.	53.	26.
10.	75.	36.
12.	90.	43.
20.	113.	53.

TABLE 11

THRESHOLD KINETIC ENERGY FOR SEVERAL BURST ENERGIES FROM ELASTIC AND INELASTIC SCATTERING ON GaAs

	Neutron Energy Threshold (MeV)	
Burst Energy (MeV)	Elastic	Inelastic
0.03	0.56	0.0
0.1	1.86	0.0
0.3	5.6	0.8
1.	18.6	6.2
2.	37.	14.2
3.	56.	22.
4.	74.	30.
5.	93.	38.
7.	130.	53.
10.	186.	77.
12.	223.	92.
20.	279.	115.

TABLE 12

INELASTIC SCATTERING CROSS SECTIONS

FOR NEUTRONS ON Si AND GaAs [a]

Energy (MeV)	Cross Section (mb) Si (n,p)	Si (n,α)	GaAs (n,p)	GaAs (n,α)
4	0.	2.7	0.	5.8
5	17.9	1.8	0.	10.1
7	201.	108.	4.1	16.7
10	262.	173.	9.9	24.6
12	248.	184.	14.0	30.1
15	193.	147.	19.9	33.3
20	49.7	32.8	17.8	25.0

[a] Natural gallium cross sections were adopted.

TABLE 13

BURST GENERATION RATE OF NEUTRONS ON Si

(Inelastic Scattering Component: Isotropic Assumption)

Neutron Energy (MeV)	Burst Energy (MeV) 0.03	0.10	0.3	1.0	2.0	3.0	5.0	7.0	10.0
4.	1.12	0.98	0.56	0.	0.	0.	0.	0.	0.
5.	0.78	0.72	0.53	0.	0.	0.	0.	0.	0.
7.	47.8	47.4	40.4	16.1	0.	0.	0.	0.	0.
10.	76.6	76.6	72.6	47.6	12.2	0.	0.	0.	0.
12.	81.5	81.5	80.2	58.6	28.2	0.	0.	0.	0.
15.	65.1	65.1	65.1	53.0	34.0	15.1	0.	0.	0.
20.	14.5	14.5	14.5	13.1	10.0	6.95	0.82	0.	0.

TABLE 14

BURST GENERATION RATE OF NEUTRONS ON GaAs

(Inelastic Scattering Component: Isotropic Assumption)

Neutron Energy (MeV)	Burst Energy (MeV)								
	0.03	0.10	0.3	1.0	2.0	3.0	5.0	7.0	10.0
4.	2.47	1.94	0.42	0.	0.	0.	0.	0.	0.
5.	4.30	3.50	1.26	0.	0.	0.	0.	0.	0.
7.	7.13	6.10	3.22	0.	0.	0.	0.	0.	0.
10.	10.6	9.43	6.21	0.	0.	0.	0.	0.	0.
12.	12.9	11.8	8.39	0.	0.	0.	0.	0.	0.
15.	14.4	13.3	10.2	0.	0.	0.	0.	0.	0.
20.	10.8	10.2	8.43	2.17	0.	0.	0.	0.	0.

FIGURE 14

BURST GENERATION RATE OF NEUTRONS ON Si

(Inelastic Scattering Component: Isotropic Assumption)

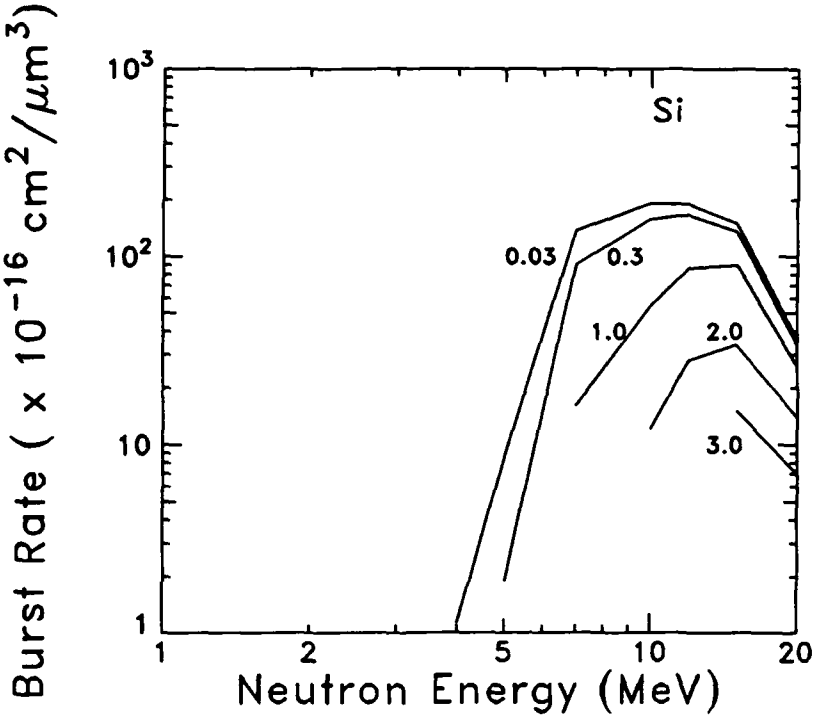

FIGURE 15

BURST GENERATION RATE OF NEUTRONS ON GaAs

(Inelastic Scattering Component: Isotropic Assumption)

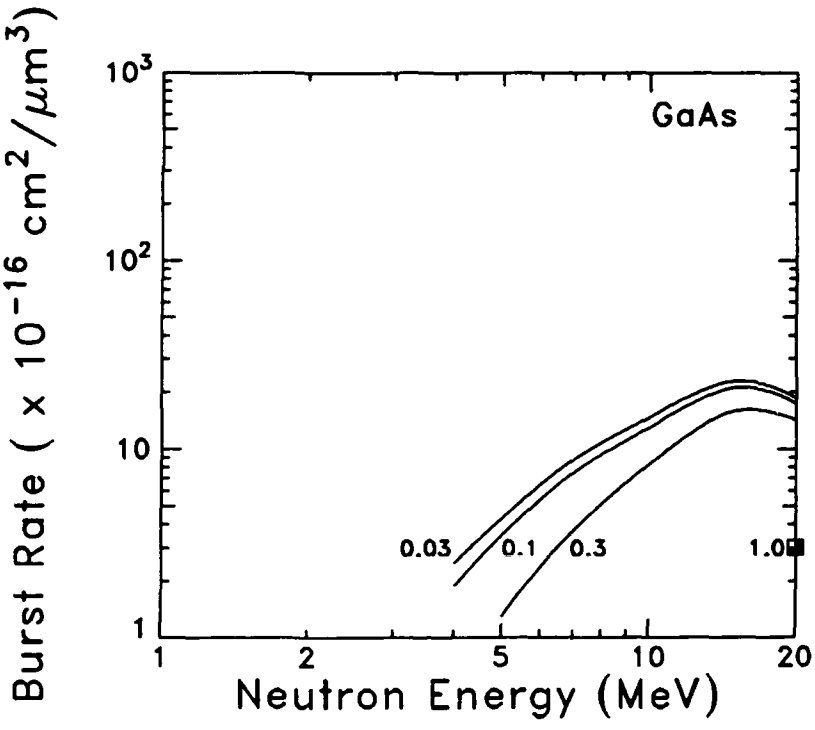

CONCLUSIONS

The Ziegler-Landford burst generation rate for neutrons on Si and on GaAs has been calculated for neutron energies between 50 MeV and 1000 MeV using the HETC program. Estimates of the burst generation rate between 1 MeV and 20 MeV have been made on the basis of ENDF elastic and inelastic cross sections, and kinematic arguments. These data are the first step toward a complete calculation of the burst generation rates in these semiconductor materials.

Significant uncertainties in the 1 MeV to 20 MeV calculation remain. Isotropic angular distributions overestimate the large-angle elastic scattering, and hence the high-energy burst rates for elastic scattering. The isotropic assumption is more appropriate for the (n,p) and (n,α) reactions. (n,nX) reactions are omitted here and should be included in a final calculation of the burst generation rates.

As stated in the introduction, a definite comparison of the relative sensitivity of Si and GaAs devices to single-event upsets depends on many factors which are outside the scope of this report. However, it may be noted that the burst generation rate in Si exceeds the burst generation rate in GaAs for $E_n < 100$ MeV and $E_b > 1$ MeV - encompassing most practical situations. For $E_n < 20$ MeV the difference is a factor of 10 or more. This difference is to be expected because GaAs is 2.5 times more massive than Si. On the basis of this analysis, one must suspect that in most environments the single-event upset susceptibility of Si is 5 or more times greater than that of GaAs.

REFERENCES

1. J.F. Ziegler and W.A. Landford, Effect of Cosmic Rays on Computer Memories, Science, **206**, 776 (1979).

2. C.H. Tsao, R. Silberberg, and J.R. Letaw, Neutron-Generated Upsets in Shielded Computer Components, IEEE TRans. Nucl. Sci., **NS-31**, 1183 (1984).

3. W.R. Frensley, Gallium Arsenide Transistors, Sci. Am., **257**, 80 (August, 1987).

4. R.E. Prael, "User Guide to the HETC Code System," (Los Alamos Laboratory draft report, 9 May 1985)

5. Brookhaven National Laboratory 1982, Guidebook for the ENDF/B-V Nuclear Data Files (EPRI NP-2510).

DTIC

FILMED

3-89